RESEARCH ARTICLE

WILEY

Hypoxia-induced hsa_circ_0000826 is linked to liver metastasis of colorectal cancer

Li Shi[1,2,3] 🆔 | Chengzhe Tao[4] | Yining Tang[5] | Yongxiang Xia[1,2,3] | Xiangcheng Li[1,2,3] | Xuehao Wang[1,2,3]

[1]Hepatobiliary Center, The First Affiliated Hospital of Nanjing Medical University, Nanjing, China

[2]Key Laboratory of Liver Transplantation, Chinese Academy of Medical Sciences, Nanjing, China

[3]NHC Key Laboratory of Living Donor Liver Transplantation, Nanjing Medical University, Nanjing, China

[4]School of Public Health, Nanjing Medical University, Nanjing, China

[5]School of Pharmacy, Nanjing Medical University, Nanjing, China

Correspondence
Xuehao Wang, Hepatobiliary Center, The First Affiliated Hospital of Nanjing Medical University, Nanjing, China.
Email: wangxh@njmu.edu.cn

Abstract

Background: hsa_circ_0000826 has been previously linked to CRC through the competing endogenous RNA network; however, the upstream driver of hsa_circ_0000826 elevation remains unknown. In this study, we aim to elucidate the effect of hypoxia-induced hsa_circ_0000826 on CRC tumorigenesis and metastasis.

Methods: RNA scope assay was used to evaluate the expression of hsa_circ_0000826 in CRC cells under hypoxia condition. The effects of hsa_circ_0000826 on phenotypes of CRC cells were evaluated through cell migration and invasion assay. The nude, AOM-DSS model mice and APC$^{Min/+}$ mice were used to investigate the relationship between circ_0000826, hypoxia, and CRC in mice. A total of 100 CRC tissue samples, as well as the paired adjacent tissues, were collected, and qRT-PCR assay was used to detect the expression of hsa_circ_0000826 in these samples.

Results: Hypoxia-induced hsa_circ_0000826 overexpression can increase the malignant phenotypes, tumor formation, and metastasis capability of CRC cells in vitro. mmu_circ_0000826 levels were significantly increased in the CRC tissues from AOM-DSS and APC mice model under hypoxia conditions. Further, the hypoxia-induced upregulation of mmu_circ_0000826 can also promote CRC tumorigenesis and liver metastasis in vivo. The expression of hsa_circ_0000826 in serum was significantly increased in CRC tissues in 100-pair of CRC and according to the adjacent normal tissues by qRT-PCR assays. Moreover, the expression levels of hsa_circ_0000826 in serum of patient with liver metastasis were significantly increased than those without metastasis.

Conclusion: Our results suggested that hsa_circ_0000826 was induced by the hypoxia in CRC, which can be a potential biomarker of CRC liver metastasis.

KEYWORDS
circRNA, CRC, hypoxia, metastasis

1 | INTRODUCTION

Colorectal cancer (CRC) is the third common malignant tumor and one leading cause of cancer-related morbidity and mortality. According to the Global Cancer Statistics, half a million people die and 1.4 million new cases occurred due to CRC annually.[1] The incidence and mortality rates of CRC are 10.2% and 9.2%, respectively.[2] After being diagnosed, the 5-year survival rate of CRC patients is about 65%.[3] Further, the progression of CRC is a process from adenoma to carcinoma and leads to metastasis eventually, preferentially (more than 70% patients) to the liver.[4] Patients with liver metastasis respond to chemotherapy resistance and have the median survival is only 6-9 months.[5] Many risk factors are associated with CRC, such as lifestyle, age, and genetic factors, and over 40 years old.[6,7]

Chemotherapy, radiation, and surgery are the common CRC conventional treatments strategy.[8] However, chemotherapy and radiotherapy have obvious side effects, which seriously affect the quality of life of CRC patients.[8] Part of the mild patients (at stage I or II) will develop to distal organ metastasis rapidly, even CRC lesion in situ has been resected.[3] Thus, investigation of the prognostic biomarkers is necessary for CRC.

CircRNAs can be divided into non-coding and coding circRNAs,[9] which are highly stable and hard to be degraded in circulation; therefore, more proper to be biomarker candidates than microRNA and lncRNAs.[10] Several circRNAs have been linked to CRC through two different mechanisms. A recent study reported that circPTK2 regulated the metastasis of CRC via the physical binding to vimentin on sites Ser38, Ser55, and Ser82.[11] In addition, competing endogenous RNA network (hsa_circ_00001666/hsa-miR-1229/CXCR5) has been reported to be an underlying mechanism of hsa_circ_00001666 involved metastasis and recurrence of CRC.[12] Xu et al found that circRNA_0001178 and circRNA_0000826 may serve as a potential biomarker for metastasis of CRC.[12] All these studies reported the association between elevated circRNA expressions in CRC tissues; however, what is the cause of increase in circRNA expression levels remains unknown.

As a solid tumor, hypoxia microenvironment in CRC is very common. Cancer cells change their gene expression patterns for adaptation and survival under hypoxic stress; therefore, the hypoxic microenvironment plays an important role in changing cancer cells' phenotype and behavior.[13] For example, tumors become more aggressive, invasive, and resistant to chemo- and radiotherapy under hypoxic conditions.[14] In addition, the non-coding RNAs profile in tumors could also be altered by hypoxia.[15] Therefore, we hypothesized that hypoxia microenvironment in CRC tissues is an upstream trigger of circRNA expression.

In this study, we aim to further clarify the association among hypoxia, hsa_circ_0000826, CRC, and its metastasis by in vivo and in vitro models. We find that hypoxia led to overexpression of hsa_circ_0000826, which subsequently promoted tumorigenesis and liver metastasis of CRC cell in tumor-bearing nude mice, AOM-DSS, and APC mice models. Besides, hsa_circ_0000826 could be a potential biomarker for prediction of CRC metastasis.

2 | MATERIALS AND METHODS

2.1 | Cell culture and in vitro experiments

Human CRC cell lines (HCT116 and SW620) and 293T cells were purchased from American Type Culture Collection (ATCC). All the CRC cells were authenticated, and no mycoplasma contamination was detected. Cell was cultured at DMEM containing 10% FBS, 100 units penicillin and streptomycin per m in a humidified atmosphere of and 95% air at 37°C. For hypoxia treatments, CRC cells were cultured in a hypoxia chamber (with 1% O_2 at 37°C) (I-Glove, BioSpherix) for 24 hours.

2.2 | RNAscope

Expression of Hsa_circ_0000826 in CRC cells was assayed with the BaseScopeTM Reagent Kit v2-RED (Advanced Cell Diagnostics) according to the manufacturer's instructions. Briefly, samples were incubated with Hsa_circ_0000826 probes at 40°C for 2 hours. After hybridization, a series of single amplification procedures were performed and finally visualized with Fast Red.[11] The number of puncta was calculated in 200 cells/group.

2.3 | Lentivirus stable transduction

Hsa_circ_0000826 KO and Hsa_circ_0000826 OEX adenovirus particles with luciferase labeling were thawed at room temperature, mixed gently, and added to 2×10^5 HCT116 or SW620 cells per well. After gently mixing, cells were incubated overnight. And cells treated with negative control lentivirus (LV-NC) were as the control. After 12 hours, culture medium was replaced with 2 mL of complete medium containing 10 μg/mL blasticidin S (Cat. No. ant-bl, Invitrogen) and replaced every 3-4 days until resistant cells can be identified. The remaining cells were collected, expanded, and then frozen down until usage. For experiments, cells were thawed and allowed to grow for three passages before use.

2.4 | Cell migration and cell invasion assays

HCT116 and SW620 cells were serum-starved by cultivation in 0.5% FBS/DMEM media for 24 hours. To analyze migration capability, 1.5×10^5 HCT116 or SW620 cells were seeded in the upper chamber in serum-free medium. To analyze invasion capability, chamber membranes were first coated with Matrigel (BD Bioscience) at a dilution of 3.3 ng/mL in medium without serum. Then, 1.5×10^5 cells

were seeded on the Matrigel in the upper chamber in serum-free medium. 10% FBS was placed as a chemo-attractant in the lower chamber. For cells cultured under normoxia, cells were incubated with complete media and exposed to 21% oxygen for 4 hours. For cells cultured under hypoxia, cells were incubated with complete media and exposed to 1% oxygen for 4 hours. After that, cell was detected in triplicate for each treatment after crystal violet staining. The absorbance was recorded at 560 nm with a microplate reader.

2.5 | Animals

All animal protocols were conducted in accordance with the guiding principles for the care and use of animals approved by the animal ethics committee of Nanjing Medical University. The APC$^{Min/+}$ mice, 5-week-old C57BL/6J mice, and nude mice were purchased from the Model Animal Research Center of Nanjing University. The animals were housed in standard pathogen-free (SPF) conditions at 24 ± 2°C, with 40%-70% relative humidity, and on a 12-hours/12-hours light/dark cycle. Water and a basal diet were given ad libitum.

2.6 | Tumor-bearing nude mice model

SW620 cells or HCT116 cells (1×10^6 cells/100 μL PBS) were subcutaneously injected into the flanks of nude mice (3 mice/group), and the mice were sacrificed 4 weeks later. The tumor, liver, and lung tissues were then harvested for further analysis.

2.7 | AOM-DSS models

To induce colitis-associated colon cancer, 5-week-old C57BL/6J mice received a single treatment of mutagen azoxymethane (AOM, Sigma-Aldrich) (10 mg/kg body weight) through intraperitoneal injection and then administered three cycles of 2% dextran sulfate sodium (DSS) in drinking water for 5 days, followed by regular drinking water for 14 days. For hypoxia treatment, mice were placed into an animal hypoxia model box and subjected to 10% O$_2$ from 8:00 AM to 8:00 PM every day during the model construction.[16,17] Mice were killed after 11 weeks.

2.8 | APC mice models

APC$^{Min/+}$ mice were exposed to normoxia or hypoxia. For hypoxia group, APC$^{Min/+}$ mice were placed into an animal hypoxia model box and subjected to 10% O$_2$ from 8:00 AM to 8:00 PM every day for 6 consecutive weeks. For normoxia group, APC$^{Min/+}$ mice were placed into an animal hypoxia model box and subjected to clean air from 8:00 AM to 8:00 PM every day. A total of 1×10^7 PFU mmu_circ_0000807 KD adenovirus were injected by tail vein per mice

every week during the model construction. All mice were killed after 6 weeks.

2.9 | HE staining and miRNA in situ hybridization (RNA-ISH)

HE staining was performed by using Hematoxylin and Eosin Staining Kit (Beyotime) according to the manufacturer's protocol. Briefly, after deparaffinization and rehydration, tissue sections were stained with hematoxylin solution for 5 minutes followed by 5 dips in 1% ethanol hydrochloride (1% HCl in 70% ethanol) and then rinsed in distilled water. Then, the sections were stained with eosin solution for 3 minutes and followed by dehydration.

The RNA-ISH was conducted as described.[18,19] Briefly, tissue sections were deparaffinized, rehydration, and treated with 10 μg/mL proteinase K at 37°C for 20 minutes. Slides were hybridized with 20-60 nmol/L double-DIG-labeled circRNA probes (Focofish) overnight at 42°C. Slides were washed in 5 × SSC, 1 × SSC, and 0.2 × SSC for 10 minutes at room temperature. Staining was performed with DAB Substrate kit (Thermo) for 30 minutes at room temperature according to the manufacturer's protocol, and then, nuclear was staining by hematoxylin for 10 minutes at room temperature. An NC-circRNA probe with scrambled sequence was used as a negative control.

2.10 | Liver metastasis mice model

A total of 5×10^5 WT or hsa_circ_0000826 overexpressed SW620 cells were injected through sub-spleen to male C57BL/6 mice to construct liver metastasis model. For hypoxia group, mice were placed into an animal hypoxia model box and subjected to 10% O$_2$ from 8:00 AM to 8:00 PM every day. For normoxia group, mice were placed into the same model box but supplied with filtered room air. 21 days later, mice were sacrificed for macroscopic examination, and liver sections were subjected to H&E staining.

2.11 | Patients and specimens

All of the samples used in this study were in compliance with the informed consent and agreement of patients as well as the institution's ethical regulations. The serum specimens and corresponding medical record information were obtained from CRC patients (n = 100) undergoing surgery in the Jiangsu Tumor Hospital in 2009. And sex- and age-matched healthy donors (n = 100) enrolled from the Nanjing Hospital of Chinese Medicine from 2016 to 2017 as control subjects, and each healthy donor had a negative diagnosis of any malignancy tumors and infectious diseases. Tumor stage was defined according to the criteria of the sixth edition of the American joint Committee on Cancer (AJCC). Detailed information of healthy donors and CRC patients is presented in Table 1.

TABLE 1 Demographic information of healthy donors and colorectal cancer (CRC) patients

Variables	Healthy donors (n = 100)		CRC patients (n = 100)	
	n	%	n	%
Age				
≤55	50	50	48	48
>55	50	50	52	52
Gender				
Male	58	58	61	61
Female	42	42	39	39
Location				
Colon			45	45
Rectum			55	55
Grade				
Low			32	32
Intermediate/High			68	68
Depth of invasion				
T1			3	3
T2			18	18
T3			20	20
T4			59	59
Lymph node metastasis				
N0			60	60
N1			40	40
Distant metastasis				
M0			85	85
M1			15	15
TNM				
I			13	13
II			40	40
III			32	32
IV			15	15

2.12 | Tissue/serum RNA isolation

Serum was separated from the venous blood within 1 hour by centrifugation at 3000 g for 10 minutes, followed by a 15-minutes high-speed centrifugation at 12 000 g to completely remove the cell debris. The total RNA from tissues and serum was extracted using TRIzol reagent (Invitrogen) and an miRNeasy Serum/Plasma Kit (Qiagen) according to the manufacturers' instructions.

2.13 | Quantitative real-time PCR analysis

For circRNA expression analysis, 1 µg total RNA was reverse-transcribed into cDNA using Quantitect RT Kits (Qiagen). And then, cDNA was analyzed using either a SYBR green-based quantitative fluorescence method (Invitrogen). GAPDH was used as a normalization control for all of the samples.

2.14 | Statistical analysis

Results are represented as mean ± SEM. RT-qPCR results were analyzed by $2^{-\Delta\Delta Ct}$ method. Differences in miRNA expression levels were analyzed by Wilcoxon rank-sum test. Probability of difference in overall survival (OS) was ascertained by Kaplan-Meier curves, and the significance was detected by a log-rank test. Multivariate Cox regression analysis was used to estimate the crude HRs, adjusted HRs, and corresponding 95% CI. Statistical analyses were performed using R, GraphPad Prism, or Stata software, and significance was set at $P < .05$.

3 | RESULTS

3.1 | Expression of hsa_circ_0000826 is upregulated in CRC cells under hypoxia condition

According to the previous study, we further analyzed the sequence of hsa_circ_0000826 and indicated its generation from back-splicing of exons 2 and 8 of its pre-mRNA ANKRD12 (Figure 1A). In addition, a murine circRNA mmu_circ_0000807 has been identified with 91% homology to hsa_circ_0000826 (Figure 1B).

To explore the role of hypoxia condition on the hsa_circ_0000826 expression, the WT and hsa_circ_0000826 knock-out (KO) SW620 and HCT116 cells were exposed to normoxia and hypoxia conditions, respectively. As shown in Figure 1C, hypoxia, a common tumor microenvironment, can significantly increase the hsa_circ_0000826 expression in HCT116 NC cells. Once the expression of hsa_circ_0000826 was ablated, the hypoxia did not exert any effects on it. The similar condition has also been observed in SW620 cells (Figure 1D). Thus, it is found that hypoxia could induce the expression levels of hsa_circ_0000826 in CRC cells.

3.2 | Hypoxia promotes the migration and invasion capacities of CRC cells in vitro through hsa_circ_0000826 induction

The migration and invasion capabilities of HCT116 and SW620 cells were evaluated by Transwell assays. As shown in Figure 2A, hypoxia condition significantly increased the migration and invasion of HCT116 cells in NC group. However, hsa_circ_0000826 KO could block the effects of hypoxia and rescue the migration and invasion of HCT116 cells to control levels. Besides, the same results were also confirmed by the results of SW620 cells in vitro
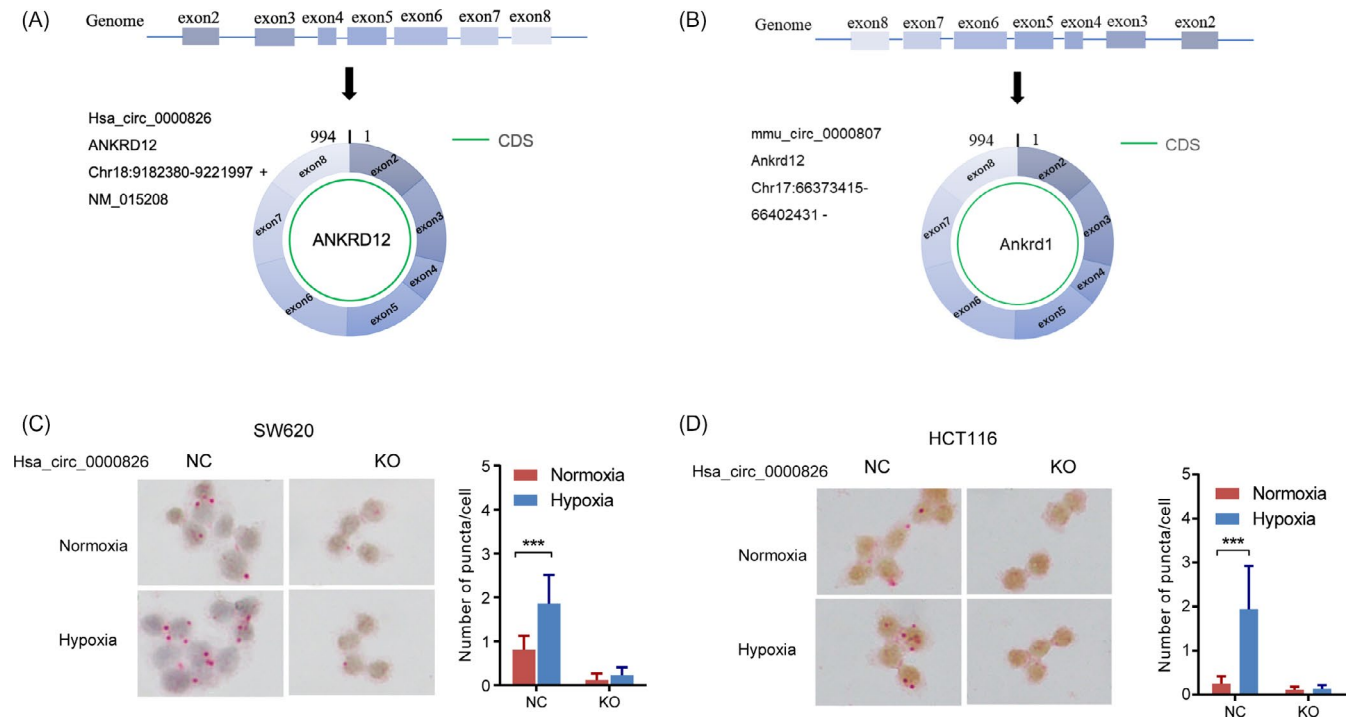
FIGURE 1 Hypoxia significantly induced expression levels of hsa_circ_0000826 in CRC cells. The circular structure of (A) hsa_circ_0000826 and (B) mmu_circ_0000807. (C) SW620 cells. (D) HCT116 cells. (Two-way ANOVA, n = 200/group, ***P < .001)
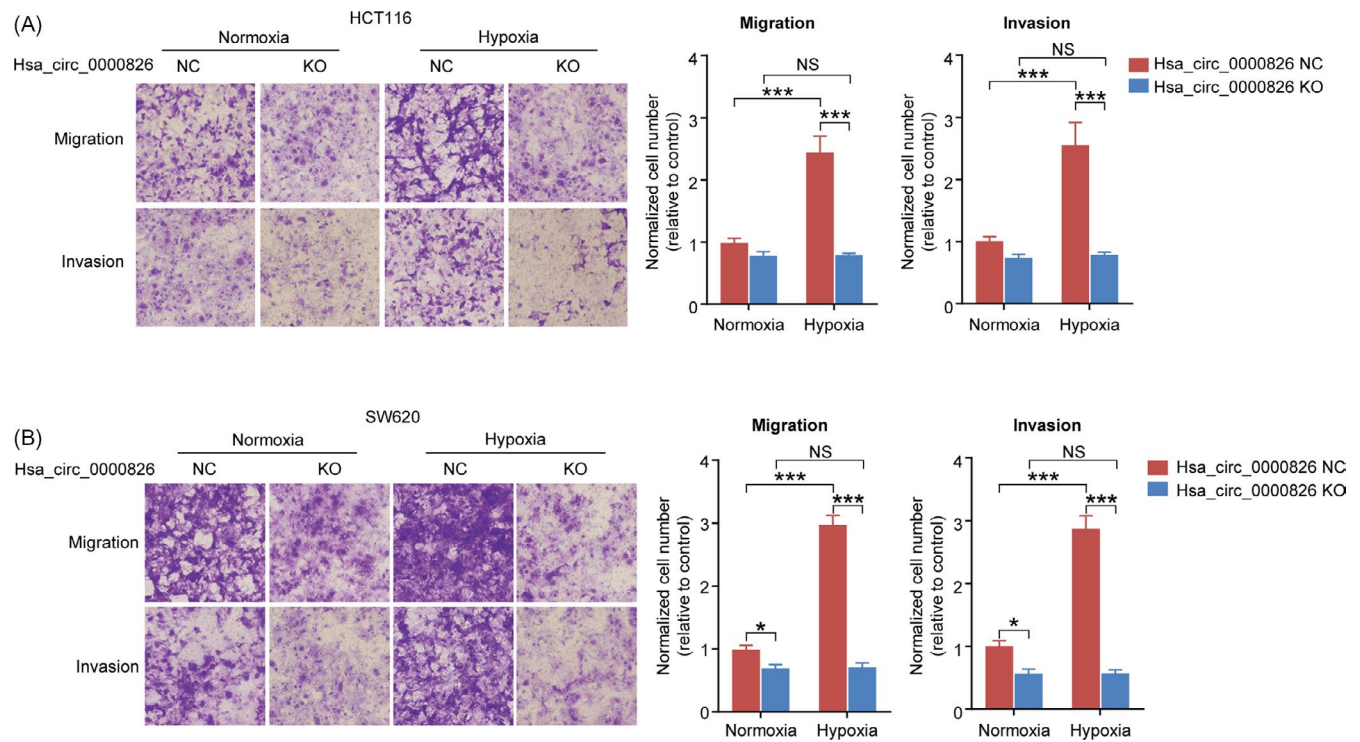
FIGURE 2 Hypoxia is associated with CRC malignant phonotype in vitro. Equal numbers of HCT116 (A) or SW620 (B) cells were subjected to migration and invasion assays. Representative images and the quantification of penetrated cells calculated from five random fields are shown (two-way ANOVA, n = 5/group, ***P < .001)

(Figure 2B). These results suggested hypoxia can increase the malignant phenotypes of CRC cells in vitro via induction of hsa_circ_0000826 expression.

3.3 | Hypoxia upregulated hsa_circ_0000826 expression is associated with tumorigenesis and metastasis of CRC cells

To further evaluate the function of hsa_circ_0000826 in vivo, luciferase-labeled HCT116 cells were subcutaneously injected into nude mice. As shown in Figure 3A, xenografts in the hypoxia-treated group showed higher tumorigenesis capability than those in the NC group. Notably, this effect was markedly reversed upon the deletion of hsa_circ_0000826. Further, the luciferase signals in tumor from the hypoxia-treated group were the highest among the three groups (Figure 3B). Besides, the luciferase in the liver and lung tissues was also detected to explore the metastasis capacities of CRC cells. Compared with the NC group, significantly higher and significantly lower luciferase activities were observed in the liver tissues from mice bearing the hypoxia-treated HCT116 cells and bearing the hsa_circ_0000826 KO HCT116 cells, respectively (Figure 3C). However, there was no obvious difference in luciferase activity was found in lung tissues among the three groups (Figure 3D). Meanwhile, the same results were also confirmed by the results of SW620 cells in vivo (Figure 3E-H). Taken together, our results suggest that hypoxia treatment of CRC cells can promote tumorigenesis and liver metastasis.

3.4 | Hypoxia-induced mmu_circ_0000807 expression was linked to CRC development in AOM-DSS model

To investigate the relationship between hypoxia and CRC in vivo, we firstly established a pharmacological model that C57BL/6J mice were subjected to azoxymethane-dextran sulfate sodium (AOM-DSS) treatment and hypoxia treatment. As shown in Figure 4A, hypoxia and AOM-DSS treatment can significantly decrease the overall survival of mice and increase colon tumor formation ratio and the number of tumors each mouse, relative to the normoxia condition. Further, hypoxia accelerated the pathological grade of tumors in murine colon than normoxia (Figure 4B). The expression levels of mmu_circ_0000807 in tumor tissues were also increased following hypoxia treatment (Figure 4C). Further analysis revealed that hypoxia condition markedly promoted mmu_circ_0000807 expression in colorectal tissues and serum and liver tissues in control and AOM-DSS murine models (Figure 4D). Taken together, our results suggest that the hypoxia microenvironment upregulated expression levels of mmu_circ_0000807, which is involved in colitis-associated colon cancer formation.

3.5 | Hypoxia upregulated expression of mmu_circ_0000807, which promote CRC tumorigenesis in APC$^{Min/+}$ mice

To further explore the relationship among hypoxia, mmu_circ_0000807 expression, and CRC development in vivo, a spontaneous colorectal
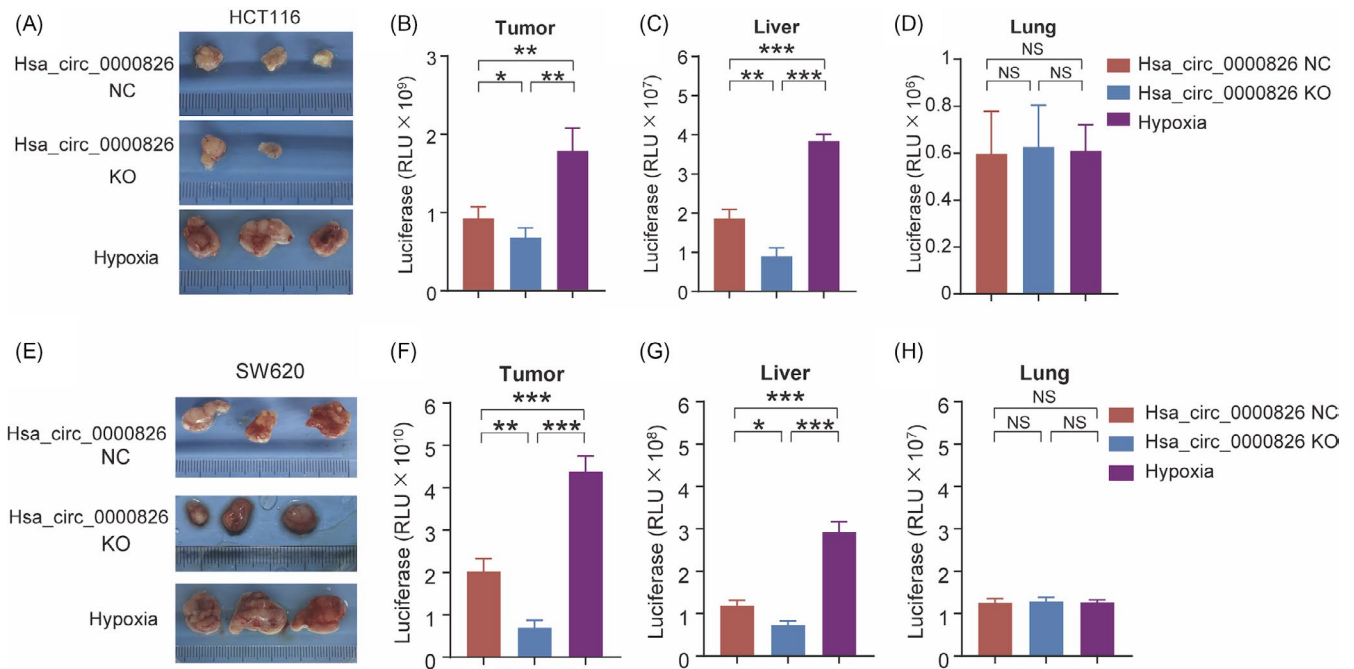
FIGURE 3 Hypoxia is associated with tumorigenesis and metastasis of CRC cells in nude mice. A, Representative images of xenografts formed by HCT116 cells in nude mice. The activities of luciferase in (B) tumor, (C) liver, and (D) lung tissues of the HCT116 cells injected nude mice. E, Representative images of xenografts formed by SW620 cells in nude mice. The activities of luciferase in (F) tumor, (G) liver, and (H) lung tissues of the SW620 cells injected nude mice (one-way ANOVA, n = 6/group; *$P < .05$, **$P < .01$, ***$P < .001$)
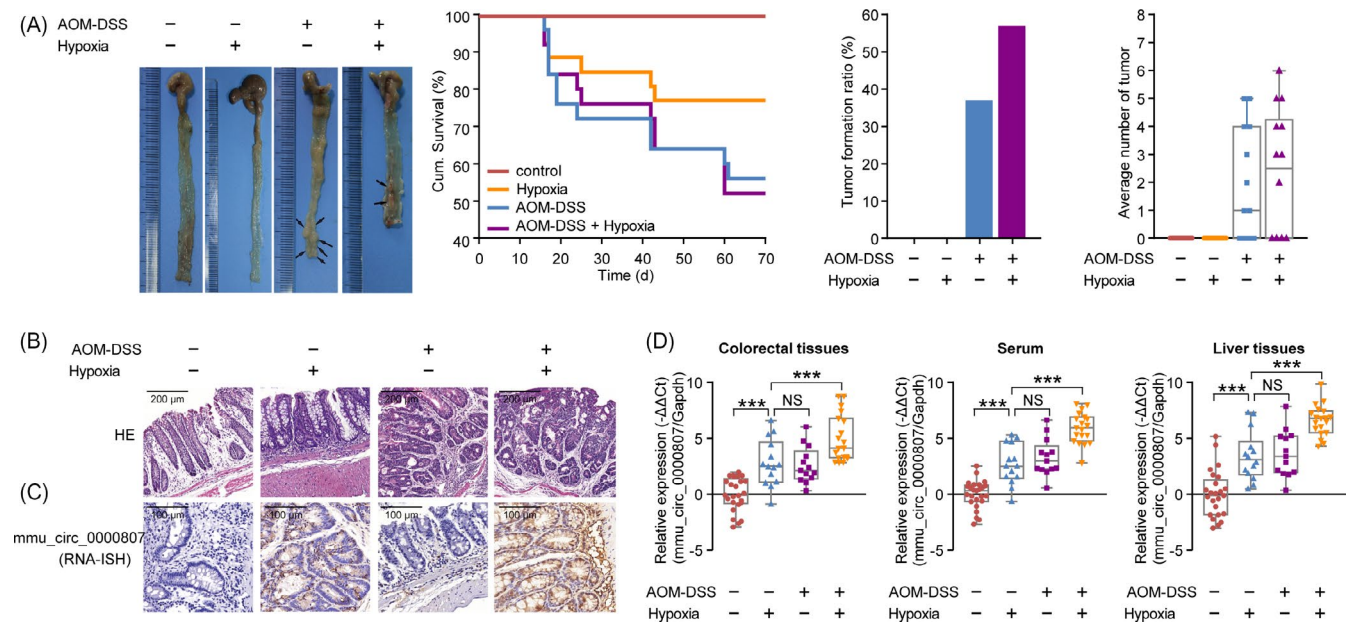
FIGURE 4 Hypoxia renders AOM-DSS-induced colonic tumorigenesis. A, Representative images of the colons from C57BL/6J mice received the indicated treatments. Kaplan-Meier curves depict the OS of C57BL/6J mice with the indicated treatments. *P* values were calculated by the log-rank test. The rate of colorectal tumor formation as well as the tumor counts. B, Representative images of H&E staining on colonic tissue sections. C, RNA-ISH analysis was applied to detect the expression of mmu_circ_0000807 in colonic tissues from mice with the indicated treatments. D, The expression levels of mmu_circ_0000807 in the colorectal, serum, and liver tissues from the indicated mice. Data are presented as $-\Delta\Delta C_t$ (one-way ANOVA, n = 3 biological replicates/group, ***P < .001)

adenoma murine model was used in our study. APC mutant (APC$^{Min/+}$) mice develop spontaneous CRC due to mutation in a tumor suppressor gene encoding adenomatous polyposis coli (APC).[20,21] The mmu_circ_0000807 knockdown or control virus was injected through the tail vein of APC$^{Min/+}$ mice to inhibit the expression of mmu_circ_0000807 in vivo. As shown in Figure 5A, the incidence of intestinal tumors and the number of tumors in each APC$^{Min/+}$ mouse were markedly increased upon hypoxic treatment. Figure 5B showed the images of pathology of colonic tumor and hypoxia with mmu_circ_0000807 NC-treated group showed severe pathological alteration. The expression levels of mmu_circ_0000807 in tumor tissues were induced in hypoxia group, but reduced by mmu_circ_0000807 KD (Figure 5C).

The qPCR analysis revealed that the tail vein injection of mmu_circ_0000807 KD adenovirus significantly decreased mmu_circ_0000807 expression both under normoxic and hypoxic conditions (Figure 5D). Furthermore, the relative abundance of mmu_circ_0000807 in the colorectal tissues and serum and liver tissues of APC$^{Min/+}$ mice under hypoxic conditions was significantly increased compared to normoxic condition (Figure 5D). Taken together, our results suggest that the hypoxia-induced mmu_circ_0000807 promoted CRC development in APC$^{Min/+}$ mice.

3.6 | hsa_circ_0000826 is a potential biomarker of CRC metastasis to liver

To investigate the relationship among hypoxia, hsa_circ_0000826 expression and CRC liver metastasis, we constructed the liver metastasis mice model by sub-spleen injection. Results showed that hypoxia treatment can facilitate the colonization of CRC cells in liver, by showing increased macroscopic neoplasm in liver than normoxia group. Based upon the pathological evaluation by H&E staining verified tumor formation in liver (Figure 6A). However, hsa_circ_0000826 KD in SW620 cells can block this effect (Figure 6A). Therefore, elevated hsa_circ_0000826 plays a role in the liver metastasis of CRC cells.

Given the association between hsa_circ_0000826 and liver metastasis of CRC revealed by in vitro and in vivo studies, we next sought to determine its potential role in human. Serum samples of CRC patients and healthy donors were used to verify the expression levels of the hsa_circ_0000826. The qPCR results confirmed serumal hsa_circ_0000826 levels were extremely higher in CRC patients (n = 100) compared to healthy donors (n = 100) (Figure 6B, *P* < .001). Meanwhile, ROC analysis results showed that hsa_circ_0000826 can accurately discriminate CRC from healthy donors (Figure 6B, *P* < .0001, AUC = 0.7778, 95% CI: 0.7157-0.8399). Furthermore, stratified analysis according to the medical record information of patients showed that hsa_circ_0000826 levels in serum samples from CRC patients with liver metastasis (n = 8) are significantly high than CRC patients without liver metastasis (n = 92) (Figure 6C, *P* < .001). And hsa_circ_0000826 could be a potential biomarker for CRC liver metastasis (Figure 6C, *P* < .001, AUC = 0.9035, 95% CI: 0.8123-0.9948). According to those results, we found that the expression level of hsa_circ_0000826 could use for auxiliary diagnosis and prognosis prediction of CRC and its liver metastasis.
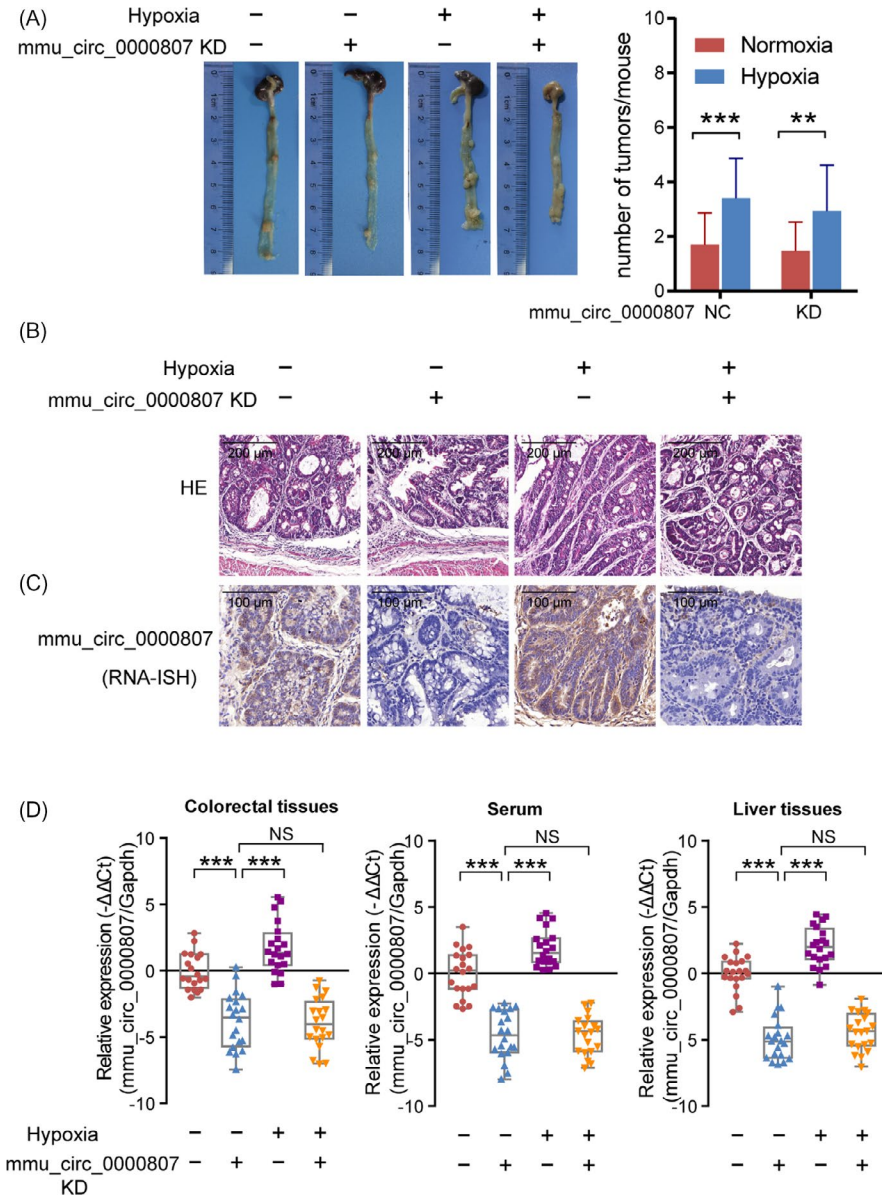
FIGURE 5 mmu_circ_0000807 triggers colorectal cancer formation in APC$^{Min/+}$ mice. A, Representative images of colons from APC$^{Min/+}$ mice that received the indicated treatments. The number of tumors/mouse were calculated ($^*P$ < .05, $^{**}P$ < .01 by two-way ANOVA). B, Colon sections from mice were subjected to H&E staining. C, mmu_circ_0000807 expression in the sections was determined by RNA-ISH analysis. D, The expression levels of hsa_circ_0000826 in the CRC, serum, and liver tissues from APC$^{Min/+}$ mice. Data are presented as $-\Delta\Delta C_t$. *P < .05, **P < .01, ***P < .001 by one-way ANOVA

4 | DISCUSSION

Liver metastasis is a common outcome and one of the critical prognostic factors for CRC. Current clinical treatments, including chemotherapy, radiotherapy, and surgery, are widely used to CRC patients in early stages, but there is limited efficiency in the treatment of CRC patients in related advanced stage.[22] It is necessary to identify novel biomarkers that can be used for early diagnosis and prognosis prediction of CRC. In the present study, we had verified that hsa_circ_0000826 can promote CRC tumorigenesis and liver metastasis in vivo and vitro. In addition, hypoxic tumor microenvironment played a vital role to induce the expression of hsa_circ_0000826 in CRC tissues. We indicated that hsa_circ_0000826 might be a biomarker for CRC and its liver metastases.

Relative to other non-coding RNAs, such as miRNAs and lncRNAs, circRNAs are novel cancer biomarker candidates due to its characteristics. The structure of circRNAs lacking 5′ or 3′ ends

is highly resistant to RNase and therefore more stable than microRNA or lncRNAs.[10] The expression of circRNAs is highly tissue- or disease-specific, reflecting the physiologic or pathologic conditions of tissues.[23] It has been showed that circRNAs participated to variety biological process through interacting with RNA binding proteins.[24] Du et al research showed that circ-Foxo3 repressing cell cycle progression through interacting with both cyclin-dependent kinase inhibitor 1A (p21) and cyclin-dependent kinase 2 (CDK2) in the mouse fibroblast NIH3T3 cell line.[25] In addition, they also found that circ-Foxo3 promoted MDM2 proto-oncogene (MDM2)-induced tumor protein P53 (p53) ubiquitination and subsequent degradation by binding to p53 and MDM2 in breast cancer cell lines.[26] Through a computational tool, it was suggested that hsa_circ_0000826 might bind with argonaute RISC component 1, 2, 3 (AGO1, 2, 3), eukaryotic translation initiation factor 4A3 (EIF4A3), insulin-like growth factor 2 MRNA binding protein 2, 3 (IGF2BP2, 3), and Lin-28 homolog A (LIN28A),[27] all of

FIGURE 6 Serum hsa_circ_0000826 is a possible marker of CRC liver metastasis. A, Representative images of murine liver and H&E staining on liver sections from SW620 cells sub-spleen injection models. Hypoxia accelerated the liver metastasis of SW620 cells in vivo, but hsa_circ_0000826 KD decelerated it. B, Levels of hsa_circ_0000826 in serum samples from healthy donors and CRC patients, as well as according receiver operating characteristic (ROC) curves. C, Levels of hsa_circ_0000826 in serum samples from CRC patients without metastasis vs CRC patients with liver metastasis, as well as according ROC curves(two-tailed t test, ***P < .001)
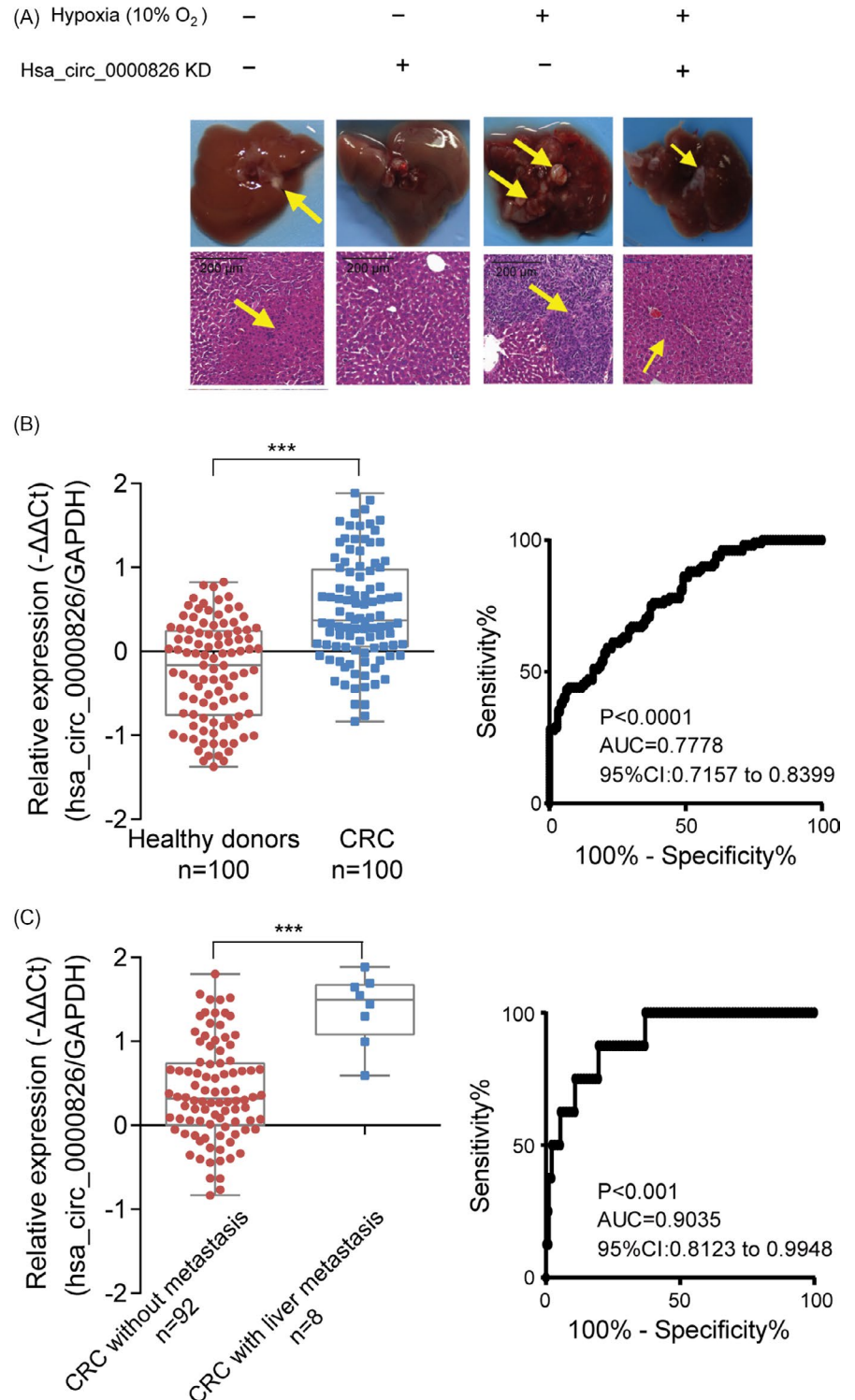
which are vital functional proteins. Taken together, we speculate that hsa_circ_0000826 might contribute to tumorigenesis and metastasis of CRC through interacting with the above RNA binding proteins.

In a recent study, Xu et al have reported that hsa_circ_0000826 is a potential biomarker of CRC metastasis; however, this conclusion was drawn based on the RNA-seq assays and bioinformatic analysis.[12] The detailed mechanism study and biological assays to validate this notion remained lack. Therefore, in the present study, we further investigated the function of hsa_circ_0000826 and our results supported the notion that hsa_circ_0000826 induction promoted tumorigenesis and metastasis of CRC both in vivo and in vitro.

Hypoxia, a common tumor microenvironment, is a hallmark for solid tumors including CRC. Tumor-hypoxia leads to dysfunction of vascularization and promotion of epithelial-to-mesenchymal transition (EMT), which resulted in cell mobility and metastasis. In

addition, hypoxia can alter cancer cell metabolism and stimulates multiple signaling networks in cancer cells. All these promoted the malignant phenotypes of cancer cells.[28] Recently, non-coding RNAs have been reported to play critical roles in the response to hypoxia in various cancers. Studies have shown that miR-10b, miR-181b, miR-155, miR-210, miR-372/373, and miR-424 were found to be upregulated under hypoxia.[29-34] As for circRNAs, the study on the links between hypoxia and their expression remains limited. One study reported that the expression of has_circRNA_403658 was induced by hypoxia and promotes bladder cancer cell growth through activation of LDHA.[35] circPTK2 was upregulated under hypoxia condition, which also associated with development of CRC.[11] Here, we supported the notion that hypoxia was an critical upstream trigger of hsa_circ_0000826 and subsequently contributed to the tumorigenesis and metastasis of CRC.

Together with the previous study, our study shed light on the application of hsa_circ_0000826 to predict the prognosis of CRC, which is also a potential therapeutic target of CRC.

CONFLICT OF INTEREST

There are no conflicts of interest to declare.

ORCID

Li Shi https://orcid.org/0000-0003-2389-7415

REFERENCES

1. Torre LA, Bray F, Siegel RL, Ferlay J, Lortet-Tieulent J, Jemal A. Global cancer statistics, 2012. *CA Cancer J Clin*. 2015;65(2):87-108.
2. Bray F, Ferlay J, Soerjomataram I, Siegel RL, Torre LA, Jemal A. Global cancer statistics 2018: GLOBOCAN estimates of incidence and mortality worldwide for 36 cancers in 185 countries. *CA Cancer J Clin*. 2018;68(6):394-424.
3. Siegel R, Desantis C, Jemal A. Colorectal cancer statistics, 2014. *CA Cancer J Clin*. 2014;64(2):104-117.
4. Rothbarth J, van de Velde CJ. Treatment of liver metastases of colorectal cancer. *Ann Oncol*. 2005;16(Suppl 2):ii144-ii149.
5. Alberts SR, Horvath WL, Sternfeld WC, et al. Oxaliplatin, fluorouracil, and leucovorin for patients with unresectable liver-only metastases from colorectal cancer: a North Central Cancer Treatment Group phase II study. *J Clin Oncol*. 2005;23(36):9243-9249.
6. Arnold M, Sierra MS, Laversanne M, Soerjomataram I, Jemal A, Bray F. Global patterns and trends in colorectal cancer incidence and mortality. *Gut*. 2017;66(4):683-691.
7. Siegel RL, Miller KD, Fedewa SA, et al. Colorectal cancer statistics, 2017. *CA Cancer J Clin*. 2017;67(3):177-193.
8. Mosinska P, Gabryelska A, Zasada M, Fichna J. Dual functional capability of dendritic cells - cytokine-induced killer cells in improving side effects of colorectal cancer therapy. *Front Pharmacol*. 2017;8:126.
9. Li Z, Ruan Y, Zhang H, Shen Y, Li T, Xiao B. Tumor-suppressive circular RNAs: Mechanisms underlying their suppression of tumor occurrence and use as therapeutic targets. *Cancer Sci*. 2019;110(12):3630-3638.
10. Memczak S, Jens M, Elefsinioti A, et al. Circular RNAs are a large class of animal RNAs with regulatory potency. *Nature*. 2013;495(7441):333-338.
11. Yang H, Li X, Meng Q, et al. CircPTK2 (hsa_circ_0005273) as a novel therapeutic target for metastatic colorectal cancer. *Mol Cancer*. 2020;19(1):13.
12. Song W, Fu T. Circular RNA-associated competing endogenous RNA network and prognostic nomogram for patients with colorectal cancer. *Front Oncol*. 2019;9:1181.
13. Zhang JX, Song W, Chen ZH, et al. Prognostic and predictive value of a microRNA signature in stage II colon cancer: a microRNA expression analysis. *Lancet Oncol*. 2013;14(13):1295-1306.
14. Selvendiran K, Bratasz A, Kuppusamy ML, Tazi MF, Rivera BK, Kuppusamy P. Hypoxia induces chemoresistance in ovarian cancer cells by activation of signal transducer and activator of transcription 3. *Int J Cancer*. 2009;125(9):2198-2204.
15. Martinez VD, Firmino NS, Marshall EA, et al. Non-coding RNAs predict recurrence-free survival of patients with hypoxic tumours. *Sci Rep*. 2018;8(1):152.
16. Omura J, Satoh K, Kikuchi N, et al. Protective roles of endothelial AMP-activated protein kinase against hypoxia-induced pulmonary hypertension in mice. *Circ Res*. 2016;119(2):197-209.
17. Ravasi G, Pelucchi S, Buoli Comani G, et al. Hepcidin regulation in a mouse model of acute hypoxia. *Eur J Haematol*. 2018;100(6):636-643.
18. Hanna JA, Wimberly H, Kumar S, Slack F, Agarwal S, Rimm DL. Quantitative analysis of microRNAs in tissue microarrays by in situ hybridization. *Biotechniques*. 2012;52(4):235-245.
19. Pena JT, Sohn-Lee C, Rouhanifard SH, et al. miRNA in situ hybridization in formaldehyde and EDC-fixed tissues. *Nat Methods*. 2009;6(2):139-141.
20. McCart AE, Vickaryous NK, Silver A. Apc mice: models, modifiers and mutants. *Pathol Res Pract*. 2008;204(7):479-490.
21. Moser AR, Luongo C, Gould KA, McNeley MK, Shoemaker AR, Dove WF. ApcMin: a mouse model for intestinal and mammary tumorigenesis. *Eur J Cancer*. 1995;31A(7-8):1061-1064.
22. Peyravian N, Larki P, Gharib E, et al. The application of gene expression profiling in predictions of occult lymph node metastasis in colorectal cancer patients. *Biomedicines*. 2018;6(1):27.
23. Salzman J, Chen RE, Olsen MN, Wang PL, Brown PO. Cell-type specific features of circular RNA expression. *PLoS Genet*. 2013;9(9):e1003777.
24. Du WW, Zhang C, Yang W, Yong T, Awan FM, Yang BB. Identifying and characterizing circRNA-protein interaction. *Theranostics*. 2017;7(17):4183-4191.
25. Du WW, Yang W, Liu E, Yang Z, Dhaliwal P, Yang BB. Foxo3 circular RNA retards cell cycle progression via forming ternary complexes with p21 and CDK2. *Nucleic Acids Res*. 2016;44(6):2846-2858.
26. Du WW, Fang L, Yang W, et al. Induction of tumor apoptosis through a circular RNA enhancing Foxo3 activity. *Cell Death Differ*. 2017;24(2):357-370.
27. Dudekula DB, Panda AC, Grammatikakis I, De S, Abdelmohsen K, Gorospe M. CircInteractome: a web tool for exploring circular RNAs and their interacting proteins and microRNAs. *RNA Biol*. 2016;13(1):34-42.
28. Muz B, de la Puente P, Azab F, Azab AK. The role of hypoxia in cancer progression, angiogenesis, metastasis, and resistance to therapy. *Hypoxia*. 2015;3:83-92.
29. Huang X, Ding L, Bennewith KL, et al. Hypoxia-inducible mir-210 regulates normoxic gene expression involved in tumor initiation. *Mol Cell*. 2009;35(6):856-867.
30. Kim CW, Oh ET, Kim JM, et al. Hypoxia-induced microRNA-590-5p promotes colorectal cancer progression by modulating matrix metalloproteinase activity. *Cancer Lett*. 2018;416:31-41.
31. Xu X, Ge S, Jia R, et al. Hypoxia-induced miR-181b enhances angiogenesis of retinoblastoma cells by targeting PDCD10 and GATA6. *Oncol Rep*. 2015;33(6):2789-2796.

32. Loayza-Puch F, Yoshida Y, Matsuzaki T, Takahashi C, Kitayama H, Noda M. Hypoxia and RAS-signaling pathways converge on, and cooperatively downregulate, the RECK tumor-suppressor protein through microRNAs. *Oncogene*. 2010;29(18):2638-2648.

33. Ghosh G, Subramanian IV, Adhikari N, et al. Hypoxia-induced microRNA-424 expression in human endothelial cells regulates HIF-alpha isoforms and promotes angiogenesis. *J Clin Invest*. 2010;120(11):4141-4154.

34. Haque I, Banerjee S, Mehta S, et al. Cysteine-rich 61-connective tissue growth factor-nephroblastoma-overexpressed 5 (CCN5)/Wnt-1-induced signaling protein-2 (WISP-2) regulates microRNA-10b via hypoxia-inducible factor-1alpha-TWIST signaling networks in human breast cancer cells. *J Biol Chem*. 2011;286(50):43475-43485.

35. Wei Y, Zhang Y, Meng Q, Cui L, Xu C. Hypoxia-induced circular RNA has_circRNA_403658 promotes bladder cancer cell growth through activation of LDHA. *Am J Transl Res*. 2019;11(11):6838-6849.